

Non-Linear Effects in Non-Kerr Spacetimes

Georgios Lukes-Gerakopoulos, George Contopoulos, and Theodoris A. Apostolatos

Abstract There is a chance that the spacetime around massive compact objects which are expected to be black holes is not described by the Kerr metric, but by a metric which can be considered as a perturbation of the Kerr metric. These non-Kerr spacetimes are also known as bumpy black hole spacetimes. We expect that, if some kind of a bumpy black hole exists, the spacetime around it should possess some features which will make the divergence from a Kerr spacetime detectable. One of the differences is that these non-Kerr spacetimes do not possess all the symmetries needed to make them integrable. We discuss how we can take advantage of this fact by examining EMRIs into the Manko-Novikov spacetime.

1 Introduction

We expect that a star which at the end of its life becomes a compact object with mass greater than three solar masses is a Kerr black hole. However, this anticipation should be somehow tested by observations.

One way to test the Kerr hypothesis is to study the gravitational wave signal produced by an inspiraling relatively light compact object (e.g., stellar) into the spacetime background of a supermassive compact object. This kind of motion is called Extreme Mass Ratio Inspiral (EMRI). Such binary systems should exist in the center of galaxies which we believe are occupied by supermassive black holes (10^5

Georgios Lukes-Gerakopoulos
Theoretical Physics Institute, University of Jena, 07743 Jena, Germany
e-mail: gglukes@gmail.com

George Contopoulos
Research Center for Astronomy, Academy of Athens, Soranou Efessiou 4, GR11527 Athens, Greece

Theodoris A. Apostolatos
Section of Astrophysics, Astronomy, and Mechanics, Department of Physics, University of Athens, Panepistimiopolis Zografos GR15783, Athens, Greece

to 10^9 solar masses). In EMRIs the lighter object basically traces the background spacetime by following approximately geodesic orbits. Ryan in [1, 2] showed that we could extract the multipole moments of the background from the gravitational wave signal, and Collins and Hughes [3] produced a perturbed Schwarzschild black hole spacetime, which they called a “bumpy” black hole spacetime, in order to provide the first tests of the Kerr hypothesis. Since then several such tests have been proposed, see e.g., [4, 5, 6] and references therein.

The bumpy black hole spacetimes are axisymmetric and stationary, but in general lack a Carter-like constant [7]. It has been shown that even in an axisymmetric stationary Newtonian potential a higher order Killing tensor giving a Carter-like constant cannot be found [8], contrary to conjectures that were initially postulated [9]. The lack of a Carter-like constant implies that the bumpy black hole systems are non-integrable, which in turn suggests that non-linear effects like chaos should be present. In a series of publications [10, 11, 12] we have studied what implications these non-linear effects will bring to a gravitational wave signal coming from an EMRI into a non-Kerr spacetime background. In the present article we present briefly these findings.

The article is organized as follows. Section 2 introduces some basic theoretical elements about a bumpy black hole spacetime and the geodesic motion in such spacetime. Section 3 discusses the non-integrability imprints of the non-Kerr background in gravitational wave signals. Our conclusions are given in section 4.

2 Theoretical elements

2.1 The Manko-Novikov spacetime

The bumpy black hole spacetime we used in [10, 11, 12] is a spacetime which belongs to the so-called Manko-Novikov (MN) metric family [13]. Manko and Novikov found an exact vacuum solution of Einstein’s equations which describes a stationary, axisymmetric, and asymptotically flat spacetime with arbitrary mass-multipole moments [13]. The MN metric subclass we used was introduced in [14] and deviates from the Kerr at all moments higher or equal to the quadrupole one. The new spacetime is characterized by one more parameter q than the ones describing a Kerr metric. Namely, the quantity q measures how much the MN quadrupole moment Q departs from the Kerr quadrupole moment $Q_{Kerr} = -S^2/M$ (that is $q = (Q_{Kerr} - Q)/M^3$), where M and S are the mass and the spin of a Kerr black hole respectively. The line element of the MN metric in the Weyl-Papapetrou cylindrical coordinates (t, ρ, φ, z) is

$$ds^2 = -f(dt - \omega d\varphi)^2 + f^{-1}[e^{2\gamma}(d\rho^2 + dz^2) + \rho^2 d\varphi^2], \quad (1)$$

where f , ω , γ are considered functions of the prolate spheroidal coordinates v, w , while the coordinates ρ, z can be expressed as functions of v, w as well. Namely,

$\rho = k\sqrt{(v^2 - 1)(1 - w^2)}$, $z = kvw$, where $k = M\frac{1-\alpha^2}{1+\alpha^2}$, $\alpha = \frac{-1+\sqrt{1-\chi^2}}{\chi}$, while χ is the dimensionless spin parameter $\chi = S/M^2$. The exact formulae of f , ω , γ are lengthy, and can be found in [14, 11].

2.2 Geodesic motion in the Manko-Novikov spacetime

The geodesic orbits of a test particle of mass μ are described as equations of motion of the Lagrangian $L = \frac{1}{2}\mu g_{\mu\nu} \dot{x}^\mu \dot{x}^\nu$, where the dots denote derivatives with respect to the proper time. The MN metric has two integrals of motion, namely the energy (per unit mass)

$$E = -\frac{\partial L}{\partial t}/\mu = f(i - \omega \phi), \quad (2)$$

and the z-component of the angular momentum (per unit mass)

$$L_z = \frac{\partial L}{\partial \phi}/\mu = f\omega(i - \omega \phi) + f^{-1}\rho^2\dot{\phi}, \quad (3)$$

The Kerr metric has one more integral of motion, the so-called Carter constant [7], thus it is an integrable system. However, the MN model lacks in general such constant (for $q = 0$ the MN metric is simply a Kerr metric), which means that MN is a non-integrable system, and therefore chaos should appear.

We can reduce the four degrees of freedom of the MN system to two, by the two integrals of motion E , and L_z , and thus, restrict the motion to the meridian plane (ρ , z). By rewriting the metric (1) we see that the motion in the meridian plane satisfies the relation

$$\frac{1}{2}(\dot{\rho}^2 + \dot{z}^2) + V_{eff}(\rho, z) = 0, \quad (4)$$

where the effective potential $V_{eff}(\rho, z)$ depends also on q , χ , E , and L_z . $V_{eff} \leq 0$ for the orbits which do not escape to infinity. In the limit $V_{eff} = 0$ eq. (4) gives $\dot{\rho} = \dot{z} = 0$; therefore, this limit determines the curve of zero velocity (CZV). Inside the CZV lie the non-escaping orbits.

In the Kerr spacetime case ($q = 0$) every non-plunging geodesic orbit confined by the CZV lies on a two dimensional torus in the phase space. On such a torus each orbit is described by two characteristic frequencies ω_1 , ω_2 . If the ratio of these frequencies ν_θ is an irrational number, the motion is quasiperiodic, and the corresponding torus is covered densely by the orbit. If the ratio is a rational number, the motion is periodic, and the corresponding torus is called resonant. A resonant torus is covered by an infinite number of periodic orbits, all having the same frequency ratio ν_θ .

By setting $q \neq 0$ we perturb the integrable system (Kerr), and the transition to the non-integrable system (MN) is described basically by two theorems: the KAM theorem, and the Poincaré-Birkhoff theorem. The first theorem states that after the perturbation most of the non-resonant tori will survive deformed. These surviving

tori are called KAM tori. The second theorem implies that from a resonant torus only a finite even number of periodic orbits will survive; half of them will be stable and the other half unstable. Around the stable orbits small islands of stability are formed, while the asymptotic manifolds emanating from the unstable periodic orbits fill a region of chaotic orbits. The above formation is known as a Birkhoff chain.

One way to study the aforementioned different structures in a non-integrable system of two degrees of freedom is to take a section through the foliation of the tori. Such section is known as a surface of section, or as a Poincaré section. Another way is provided by the frequency ratio ν_θ , by which we can detect the different types of orbits and it is known as the rotation number (e.g., [15]). If ν_θ corresponds to an irrational number, we have a KAM curve; if it corresponds to a rational number, we are on a Birkhoff chain of islands of stability; if the value of ν_θ is indefinite, and does not correspond to a particular number, then the orbit is chaotic.

3 Non-integrability imprints on the gravitational wave signal

3.1 The plateau effect of the resonances

One possible imprint of the non-integrability of a bumpy black hole spacetime on a gravitational wave signal is the effect of the resonances. The left panel of Fig. 1 shows a part of the surface of section $z = 0$ ($z > 0$) of a MN spacetime for the parameter set $E = 0.95$, $Lz = 3M$, $\chi = 0.9$, $q = 0.95$. One's first impression might be that the surface of section indicates an integrable system, because no straightforward signs of chaos are prominent. However, the islands of stability (left panel of Fig. 1) implies the existence of Birkhoff chains, which in turn indicates that chaos is also present.

If we take initial conditions along a straight line in the phase space, like the $\dot{\rho} = 0$ line starting from the center \mathbf{u}_0 of the main island of stability shown in the left panel of Fig. 1, and evaluate the rotation number for each of these initial conditions, then we get a rotation curve (right panel of Fig. 1). This curve seems to be smooth and strictly monotonic (in a Kerr spacetime this is the case), however a more detailed look reveals that this is not true. At the resonances, plateaus appear. For instance in the embedded plot of the right panel of Fig. 1, we can see a plateau at the 2/3 resonance. This happens because all the orbits belonging to the same chain of islands of stability share the same rotation number, i.e., the same frequency ratio. Such plateaus do not appear in the case of a Kerr metric.

However, geodesic orbits are simply an approximation of real EMRI orbits. A more realistic approximation demands the inclusion of the radiation reaction. Since there are no reliable computations describing the radiation reaction in a bumpy black hole spacetime, we used the same trick as the authors of [14]. Namely, we used the hybrid approximative method [16] (eqs. (44), (45) in [16]), where we added by hand

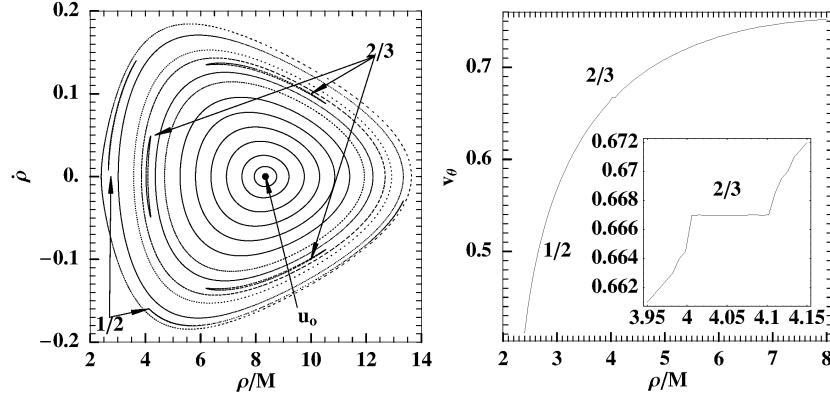


Fig. 1 The left panel shows a part of the surface of section in the plane $(\rho, \dot{\rho})$ focusing on the main island of stability, where \mathbf{u}_0 indicates the center of the main island. The right panel shows the rotation number along the line $\dot{\rho} = 0$ (starting from \mathbf{u}_0 and moving leftwards) on the surface of section shown in the left panel. Embedded in the right panel is a detail of the rotation curve around the $2/3$ -resonance. The parameters used are $E = 0.95$, $L_z = 3M$, $\chi = 0.9$, $q = 0.95$.

the anomalous quadrupole moment q to the χ^2 terms. Furthermore, we assumed a constant rate of energy and angular momentum loss due to gravitational radiation.

We applied the aforementioned scheme for a mass ratio $\mu/M = 8 \times 10^{-5}$, evolved initial conditions near the $2/3$ resonance, and found that the plateau also appears when we calculate the rotation number as a function of the coordinate time (left panel of Fig. 2). This phenomenon was tested for several initial conditions near the $2/3$ resonance and for each of them we estimated the time Δt_r that the inspiraling non-geodesic orbit stayed in the resonance (right panel of Fig. 2). The mean time of these plateaus is approximately $5 \times 10^4 M$, which corresponds roughly to a week for a supermassive compact object of the size of the one lying at the center of the Milky Way.

3.2 The Beacon effect of stickiness

If we focus more on the chaotic aspect of the Birkhoff chains, another effect could be detected in gravitational waves coming from an EMRI in a bumpy black hole spacetime background. This effect is connected with the phenomenon of stickiness [15]. The stickiness phenomenon concerns chaotic orbits which for various reasons stick for a long time interval in a region close to regular orbits. Therefore, their behavior in the frequency spectrum might resemble that of the regular orbits they are close to, before they depart from that region.

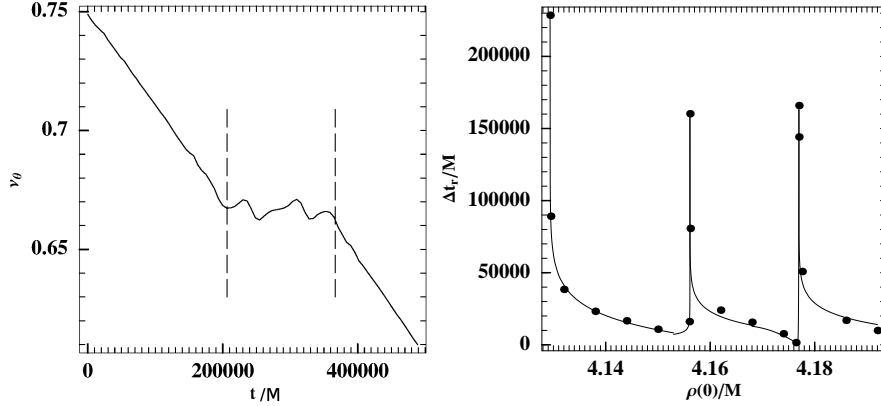


Fig. 2 The left panel shows the evolution of the ratio ν_θ as a function of the coordinate time t for a non-geodesic orbit. The vertical dashed lines demarcate the time intervals that the non-geodesic orbit spends in the interior of the $2/3$ -resonance. The right panel shows the time Δt_r needed by non-geodesic orbits to cross the chain of islands belonging to the $2/3$ -resonance as a function of their initial conditions $\rho(0)$ along the line $\dot{\rho} = 0$, $z = 0$. The parameters used are $\mu/M = 8 \times 10^{-5}$, $q = 0.95$, $\chi = 0.9$, $E(0) = 0.95$, $L_z(0) = 3M$, where $E(0)$, $L_z(0)$ are the initial values of E and L_z respectively.

In the left panel of Fig. 3 we see a detail of the surface of section near the resonance $2/7$. The stickiness appears in the region where chaotic orbits (scattered points on the surface of section) are confined by regular orbits. Even though their true character is detected by the rotation number, because ν_θ varies in the corresponding regions (right panel of Fig. 3), in the frequency spectrum the phenomenology might be more complicated. Namely, while a chaotic orbit stays near a regular orbit we might get a signal, i.e., distinct characteristic frequencies; when the orbit moves to a more prominent chaotic layer the frequency peaks in the signal will dissolve leaving only noise instead of a signal; later on when the orbit returns near a regular orbit the signal shall reappear, and so on. This effect resembles a beacon, where the signal appears and disappears.

4 Conclusions

The resonance and the stickiness effect are generic characteristics of the geodesic motion in any non-integrable Hamiltonian system describing a stationary and axisymmetric spacetime background which is an axially symmetric perturbation of the Kerr spacetime. Therefore, they should be in principle detectable in a gravitational wave signal coming from an EMRI into a non-Kerr metric.

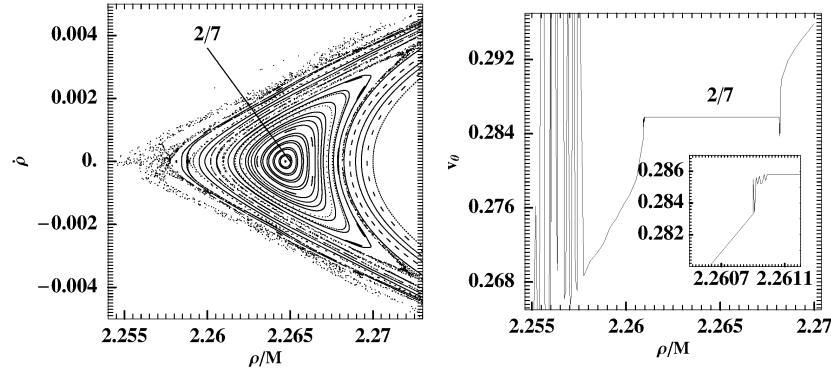


Fig. 3 The left panel shows a detail of the surface of section near an island $2/7$. The right panel shows the rotation curve along the $\dot{\rho} = 0$ line of the surface of section presented in the left panel. Embedded in the right panel is the irregular variation of the rotation number just outside the left side of the $2/7$ -plateau. This irregular behavior is due to the chaotic layer surrounding the corresponding island. The parameters used are $E = 0.95$, $L_z = 2.995 M$, $\chi = 0.9$, $q = 0.95$.

Acknowledgements: G. L-G is supported by the DFG grant SFB/Transregio 7.

References

1. F.D. Ryan, *Gravitational waves from the inspiral of a compact object into a massive, axisymmetric body with arbitrary multipole moments*, Phys. Rev. D **52**, 5707 (1995)
2. F.D. Ryan, *Accuracy of estimating the multipole moments of a massive body from the gravitational waves of a binary inspiral*, Phys. Rev. D **56**, 1845 (1997)
3. N.A. Collins, S.A. Hughes, *Towards a formalism for mapping the spacetimes of massive compact objects: Bumpy black holes and their orbits*, Phys. Rev. D **69**, 124022 (2004)
4. P. Amaro-Seoane, S. Aoudia, S. Babak, et al., *Low-frequency gravitational-wave science with eLISA/NGO*, Class. Quantum Grav. **29**, 124016 (2012)
5. C. Bambi, *Testing the Kerr black hole hypothesis*, Mod. Phys. Lett. A **26**, 2453 (2011)
6. T. Johannsen, *Testing the no-hair theorem with Sgr A**, Adv. Astron. **2012**, 486750 (2012)
7. B. Carter, *Global Structure of the Kerr Family of Gravitational Fields*, Phys. Rev. **174**, 1559 (1968)
8. C. Markakis, *Constants of motion in stationary axisymmetric gravitational fields*, ArXiv e-prints [arXiv:1202.5228 [astro-ph.SR]] (2012)
9. J. Brink, *Formal solution of the fourth order Killing equations for stationary axisymmetric vacuum spacetimes*, Phys. Rev. D **84**, 104015 (2011)
10. T.A. Apostolatos, G. Lukes-Gerakopoulos, G. Contopoulos, *How to observe a non-Kerr spacetime using gravitational waves*, Phys. Rev. Lett. **103**, 111101 (2009)
11. G. Lukes-Gerakopoulos, T.A. Apostolatos, G. Contopoulos, *Observable signature of a background deviating from the Kerr metric*, Phys. Rev. D **81**, 124005 (2010)
12. G. Contopoulos, G. Lukes-Gerakopoulos, T.A. Apostolatos, *Orbits in a non-Kerr dynamical system*, Int. J. Bifurcat. Chaos **21**, 2261 (2011)

13. V.S. Manko, I.D. Novikov, *Generalizations of the Kerr and Kerr-Newman metrics possessing an arbitrary set of mass-multipole moments*, *Class. Quantum Grav.* **9**, 2477 (1992)
14. J.R. Gair, C. Li, I. Mandel, *Observable properties of orbits in exact bumpy spacetimes*, *Phys. Rev. D* **77**, 024035 (2008)
15. G. Contopoulos, *Order and chaos in dynamical astronomy*. Astronomy and astrophysics library (Springer, 2002)
16. J.R. Gair, K. Glampedakis, *Improved approximate inspirals of test bodies into Kerr black holes*, *Phys. Rev. D* **73**(6), 064037 (2006)